Materials Science, *Vol. 21*, *No. 2*, *2003*

Spin crossover in a supramolecular Fe^{II}–Fe^{III} system*

HIROMI OHTA[1], YUKINARI SUNATSUKI[1], YUICHI IKUTA[2], NAOHIDE MATSUMOTO[2], SEIICHIRO IIJIMA[3], HARUO AKASHI[4], TAKASHI KAMBE[5], MASAAKI KOJIMA[1**]

[1]Department of Chemistry, Faculty of Science, Okayama University, Tsushima, Okayama 700-8530, Japan

[2]Department of Chemistry, Faculty of Science, Kumamoto University, Kumamoto 860-8555, Japan

[3]National Institute of Advanced Industrial Science and Technology, Tsukuba 305-8566, Japan

[4]Research Institute of Natural Sciences, Okayama University of Science, Ridai-cho, Okayama 700-0005, Japan

[5]Department of Physics, Faculty of Science, Okayama University, Tsushima, Okayama 700-8530, Japan

The structure of $[Fe^{II}(H_3L)](ClO_4)_2 \cdot 3H_2O$, where H_3L is a tripodal hexadentate ligand derived from the 1:3 condensation of tris(2-aminoethyl)amine and 4-formylimidazole, has been determined by X-ray crystallography at 113 and 293 K. A spin transition was inferred from the Fe–N bond distances. The temperature dependence of the magnetic susceptibility revealed that the complex undergoes a gradual spin transition in the temperature range of 150–270 K. A mixed-valence complex, $[Fe^{II}(H_3L)][Fe^{III}(L)](BF_4)_2 \cdot 1.5H_2O$, was prepared by the controlled deprotonation of the protonated species, $[Fe^{II}(H_3L)](BF_4)_2 \cdot 1.5H_2O$, under aerobic conditions, and the X-ray structure was determined at 293 K. Two species, $[Fe^{II}(H_3L)]^{2+}$ and $[Fe^{III}(L)]$, are linked by imidazole–imidazolate (NH···N) hydrogen bonds to form a puckered sheet structure. Magnetic susceptibility measurements and Mössbauer spectra provided an evidence for spin-crossover at both the Fe^{II} and Fe^{III} sites. There are three accessible electronic states: (LS Fe^{II}–LS Fe^{III}), (HS Fe^{II}–LS Fe^{III}), and (HS Fe^{II}–HS Fe^{III}) that occur in passing from lower to higher temperatures.

Keywords: *spin crossover; hydrogen bonds; tripodal ligand*

1. Introduction

Increasing attention has been paid to the synthesis of compounds showing bistable behaviour, because they can be used as molecular switches in electronic devices [1].

---

* The paper was presented at the 13th Winter School on Coordination Chemistry, Karpacz, Poland, 9–13 December, 2002.

** Corresponding author, e-mail: kojima@cc.okayama-u.ac.jp.

The phenomenon of spin crossover represents one of the most spectacular examples of molecular bistability [2]. Cooperative spin crossover, where an interaction between spin crossover sites occurs within a crystal lattice, is the dominant factor governing bistability [3]. A polymeric strategy has been widely used to obtain a spin crossover material that has a large cooperative effect, where the spin crossover sites are linked together by chemical bridges to form a linear chain structure [1, 4]. Mononuclear spin-crossover Fe^{II} compounds exhibiting strong intermolecular interactions, such as hydrogen bonding [5, 6] and π–π stacking [3, 7, 8] interactions are rather scarce, and the requirements for sharp spin transition are difficult to control. Our strategy controlling a spin crossover behaviour is based on the formation of an extended two-dimensional (2D) sheet structure, which arises from intermolecular hydrogen bonds.

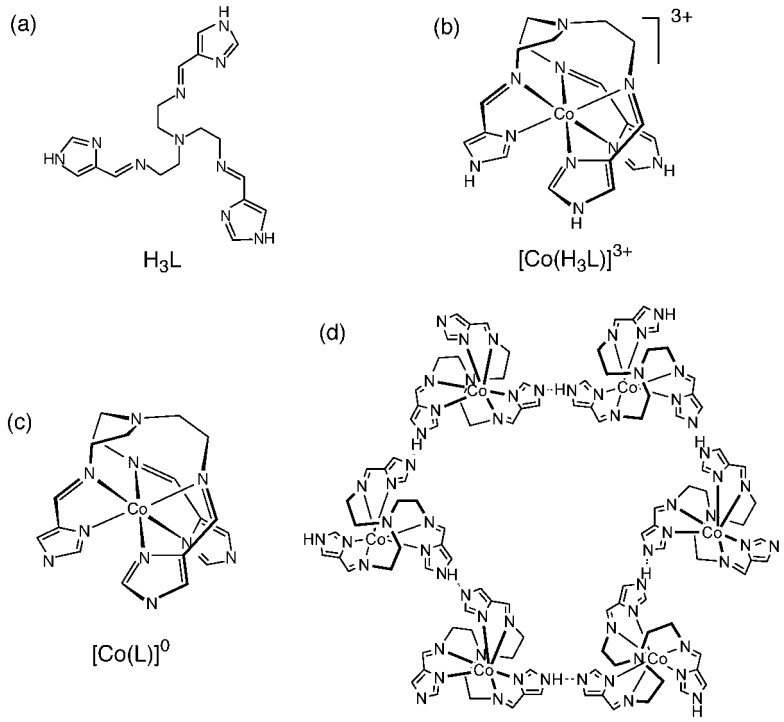

Fig. 1. The tripodal H_3L ligand (a); the structure of $[Co^{III}(H_3L)]^{3+}$ (b); the structure of $[Co^{III}(L)]^0$ (c) and the hexanuclear structure as repeating unit of the 2D sheet constructed from intermolecular imidazole–imidazolate hydrogen bonds between $[Co^{III}(H_3L)]^{3+}$ and $[Co^{III}(L)]^0$ (d)

We have focused on the homochiral 2D extended network structure of $[Co^{III}(H_3L)]$-$[Co^{III}(L)]X_3$ [9], arising from the intermolecular imidazole–imidazolate hydrogen bonds between $[Co^{III}(H_3L)]^{3+}$ and $[Co^{III}(L)]^0$, where H_3L denotes a tripodal hexadentate ligand derived from the 1:3 condensation of tris(2-aminoethyl)amine and 4-formylimidazole (Fig. 1). This formally hemi-deprotonated species, $[Co^{III}(H_{1.5}L)]X_{1.5}$ (i.e., $[Co^{III}(H_3L)]$-$[Co^{III}(L)]X_3$), was prepared by the controlled deprotonation of the protonated species,

$[Co^{III}(H_3L)]X_3$. A similar synthetic procedure for the iron(II) species gave a mixed-valence Fe^{II}–Fe^{III} spin crossover compound with the formula $[Fe^{II}(H_3L)][Fe^{III}(L)](BF_4)_2 \cdot 1.5H_2O$ (**3**). This paper reports on the preparation, structure, and magnetic properties of **3** and related complexes.

2. Experimental

2.1. Preparation of $[Fe^{II}(H_3L)](ClO_4)_2 \cdot 3H_2O$ (1), $[Fe^{II}(H_3L)](BF_4)_2 \cdot 1.5H_2O$ (2), and $[Fe^{II}(H_3L)][Fe^{III}(L)](BF_4)_2 \cdot 1.5H_2O$ (3)

The H_3L ligand was prepared by the reaction of tris(2-aminoethyl)amine and 4-formylimidazole in a 1:3 molar ratio in methanol. The solution containing the H_3L ligand was then mixed with a methanol solution of $FeCl_2 \cdot 4H_2O$ in a 1:1 molar ratio. The mixture was heated under reflux for 30 min, and after cooling, $NaClO_4$ (3 equiv) was added to yield a yellow-orange precipitate. The precipitate was filtered and re-crystallized from methanol containing a small volume of ascorbic acid. Found: C, 31.61; H, 4.30; N, 20.59%. Calc. for $C_{18}H_{30}Cl_2Fe_1N_{10}O_{11}$= $[Fe^{II}(H_3L)](ClO_4)_2 \cdot 3H_2O$ (**1**): C, 31.37; H, 4.39; N, 20.32. $[Fe^{II}(H_3L)](BF_4)_2 \cdot 1.5H_2O$ (**2**) was isolated by the addition of excess $NaBF_4$ to a methanol solution of $[Fe^{II}(H_3L)]Cl_2$. Found: C, 34.24; H, 4.62; N, 21.52%. Calc. for $C_{18}H_{27}B_2F_8Fe_1N_{10}O_{1.5}$: C, 33.95; H, 4.27; N, 21.99.

To a warm methanol solution of **2**, an aqueous solution of NaOH (1:1 molar ratio) was added under aerobic conditions. The colour of the solution gradually changed from yellow to dark green, and a mixed-valence complex with the chemical formula $[Fe^{II}(H_3L)][Fe^{III}(L)](BF_4)_2 \cdot 1.5H_2O$ (**3**) was produced. Found: C, 40.25; H, 4.61; N, 26.12%. Calc. for $C_{36}H_{48}B_2F_8Fe_2N_{20}O_{1.5}$: C, 40.40; H, 4.52; N, 26.18%.

2.2. Physical measurements

The samples' magnetic susceptibilities were measured using a Quantum Design MPMS5 and MPMS2 SQUID susceptometer in the temperature range of 2–350 K under an applied magnetic field of 1 T. Mössbauer spectra were recorded using a Wissel 1200 spectrometer and a proportional counter. A $^{57}Co(Rh)$ radioactive source moving in a constant acceleration mode was used. The isomer shifts were calculated relative to a metallic iron foil.

2.3. X-ray crystal structure analysis of $[Fe^{II}(H_3L)](ClO_4)_2 \cdot 3H_2O$ (1) and $[Fe^{II}(H_3L)][Fe^{III}(L)](BF_4)_2 \cdot 1.5H_2O$ (3)

X-ray measurements were taken using a Rigaku RAXIS-IV imaging plate area detector employing graphite monochromated Mo K_α radiation (λ = 0.71073 Å). The structure was

solved using direct methods, and was refined using full-matrix least-squares procedures employing the CrystalStructure crystallographic software package [10]. Crystal data at 113 K for **1**: Formula $[Fe^{II}(H_3L)](ClO_4)_2{\cdot}3H_2O = C_{18}H_{30}Cl_2FeN_{10}O_{11}$, Fw = 689.25, orange, prism, trigonal, space group *R*32(h) (No. 155), $a = b = 11.851(1)$, $c = 34.2177(2)$ Å, $V = 4161.7(5)$ Å^3, $Z = 6$, $D_{calc} = 1.650$ g·cm^{-3}, $\mu = 0.810$ mm^{-1}, No. of reflections measured = 1228, unique reflections = 1228, $R = 0.163$ [1152 $I > 2\sigma(I)$], $R_w = 0.212.(2)$. Crystal data at 293 K for **1**: Formula $[Fe^{II}(H_3L)](ClO_4)_2{\cdot}3H_2O = C_{18}H_{30}Cl_2FeN_{10}O_{11}$, Fw = 689.25, orange, prism, trigonal, space group *R*32(h) (No. 155), $a = b = 12.0774(9)$, $c = 35.8111(2)$ Å, $V = 4523.7(5)$ Å^3, $Z = 6$, $F(000) = 2136$, $D_{calc} = 1.518$ g cm^{-3}, $\mu = 0.810$ mm^{-1}, No. of reflections measured = 1322, Unique reflections = 1322, $R = 0.163$ [1152 $I > 2\sigma(I)$], $R_w = 0.168$. The systematic extinction of the X-ray diffraction data at both temperatures suggested either the space group *R*32 or *R*3*m*. The structure was well determined when *R*32 was assumed, while we could not determine the structure when *R*3*m* was assumed. Thus, the space group *R*32 was selected.

Crystal data for **3** at 293 K: Formula $[Fe^{II}(H_3L)][Fe^{III}(L)](BF_4)_2{\cdot}1.5H_2O = C_{36}H_{48}B_2F_8Fe_2N_{20}O_{1.5}$, Fw = 1070.2, dark green, block, trigonal, space group *P*3 (No. 143), $a = b = 11.9074(2)$, $c = 28.5477(4)$ Å, $V = 3505.38(8)$ Å^3, $Z = 6$, $D_{calc} = 1.521$ g·cm^{-3}, No. of reflections measured = 19023, unique reflections = 5188 ($R_{int} = 0.033$), $R = 0.080$ [7005 $I > 2\sigma(I)$], and $R_w = 0.117$.

3. Results and discussion

3.1. Preparation, structure and magnetic properties of $[Fe^{II}(H_3L)](ClO_4)_2{\cdot}3H_2O$ (1)

The tripodal H_3L ligand was prepared by the reaction of tris(2-aminoethyl)amine and 4-formylimidazole in a 1:3 molar ratio in methanol. This ligand solution was used without isolation for the synthesis of the iron(II) complexes. The $[Fe^{II}(H_3L)](ClO_4)_2{\cdot}3H_2O$ (**1**) complex was obtained as yellow-orange crystals by mixing the ligand solution, $FeCl_2{\cdot}4H_2O$, and $NaClO_4$ in a 1:1:3 molar ratio. The crude product was purified by recrystallization from methanol containing a small amount of ascorbic acid as a reducing agent.

The structure of **1** was determined by X-ray crystallography at 113 and 293 K. Figure 2 shows an ORTEP drawing for the cation of complex **1**. The iron atom is in an approximately octahedral environment composed of three facially co-ordinated imine nitrogen atoms and three imidazole nitrogen atoms. At 293 K, the average Fe–N(imine) and Fe–N(imidazole) bond distances are 2.18(2) and 2.20(2) Å, respectively. These values are typical of a high-spin (HS) iron(II) ion [3, 11, 12]. At 113 K, the Fe–N bond distances shorten by about 0.2 Å versus those at 293 K: the average

Fe–N(imine) and Fe–N(imidazole) bond distances are 2.02(2) and 1.98(1) Å, respectively, suggestive of a low-spin (LS) Fe^{II} species.

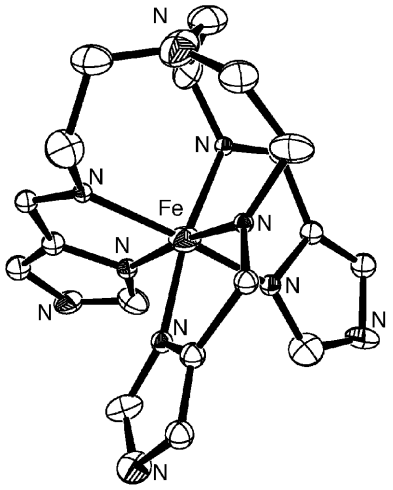

Fig. 2. An ORTEP drawing of the cation of $[Fe^{II}(H_3L)](ClO_4)_2 \cdot 3H_2O$ (**1**) showing the 50% probability ellipsoid. The hydrogen atoms have been omitted for clarity

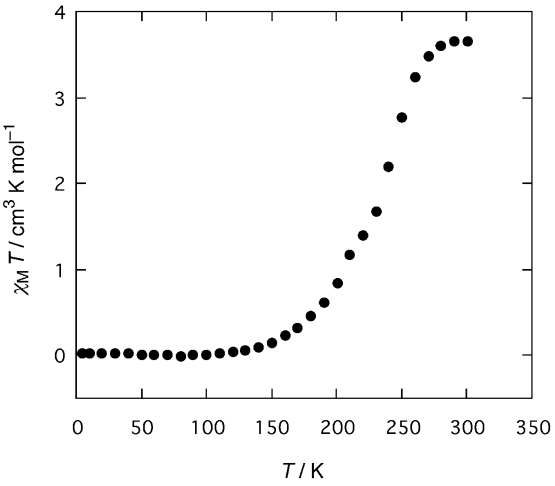

Fig. 3. A plot of $\chi_M T$ versus T for $[Fe^{II}(H_3L)](ClO_4)_2 \cdot 3H_2O$ (**1**)

The magnetic properties of **1** are shown in Fig. 3 in the form of a $\chi_M T$ versus T curve, in which χ_M is the molar magnetic susceptibility and T is the absolute temperature. Complex **1** shows a spin transition in the temperature range of 150–270 K. Above 270 K, the complex is in the HS state, while below 150 K, it is in the LS state. These results are consistent with the X-ray structure study.

3.2. Preparation, structure and properties of $[Fe^{II}(H_3L)][Fe^{III}(L)](BF_4)_2 \cdot 1.5H_2O$ (3)

The reaction of $[Fe^{II}(H_3L)](BF_4)_2 \cdot 1.5H_2O$ (**2**) with NaOH (1:1 ratio) under aerobic conditions yielded a dark green, mixed-valence complex, $[Fe^{II}(H_3L)][Fe^{III}(L)](BF_4)_2 \cdot 1.5H_2O$ (**3**). Deprotonation and oxidation of $[Fe^{II}(H_3L)]^{2+}$ took place during the course of the reaction to generate the fully-deprotonated species $[Fe^{III}(L)]$, which functions as a component of the mixed valence complex, **3**. Thus, this reaction is an example of a proton-coupled electron transfer reaction [13].

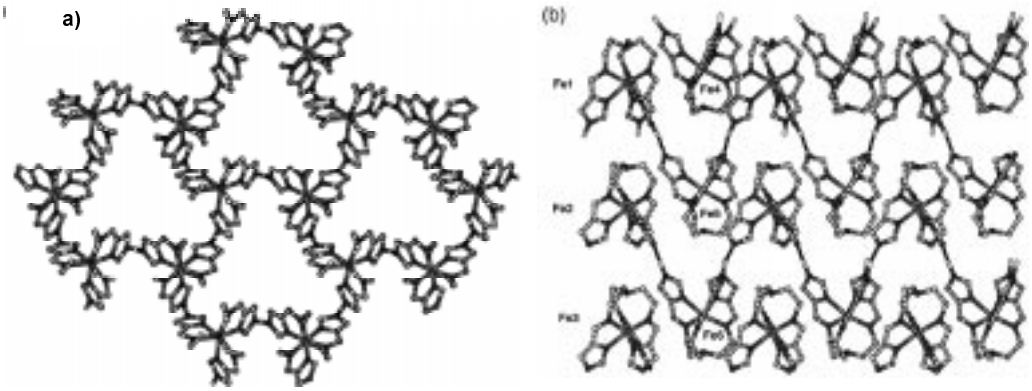

Fig. 4. The X-ray crystal structure of $[Fe^{II}(H_3L)][Fe^{III}(L)](BF_4)_2 \cdot 1.5H_2O$ (**3**) showing the homochiral 2D sheet structure formed by hydrogen bonds between $[Fe^{II}(H_3L)]^{2+}$ and $[Fe^{III}(L)]^{0}$. The counter ions and the water molecules have been omitted for clarity; a) a top view showing the sheet structure in which the same enantiomers are linked by intermolecular imidazole–imidazolate hydrogen bonds; b) a side view showing that there are three types of layers: the first layer consists of HS $Fe^{II}1$ and HS $Fe^{II}4$ complexes; the second layer consists of LS $Fe^{III}2$ and LS $Fe^{III}5$ complexes; and the third layer consists of HS $Fe^{III}3$ and HS $Fe^{II}6$ complexes. The HS $Fe^{II}1$ and LS $Fe^{III}5$, LS $Fe^{III}2$ and HS $Fe^{II}6$, and HS $Fe^{III}3$ and HS $Fe^{II}4$ complexes are connected by hydrogen bonds

The crystal structure was determined from single-crystal X-ray analysis at 293 K. The structure consists of three protonated $[Fe^{II}(H_3L)]^{2+}$ ions, three deprotonated $[Fe^{III}(L)]$ species, six BF_4^- counter anions, and four and a half water molecules of crystallization. The structures of the component complexes, $[Fe^{II}(H_3L)]^{2+}$ and $[Fe^{III}(L)]$, are similar to that of **1**. Adjacent $[Fe^{II}(H_3L)]^{2+}$ and $[Fe^{III}(L)]$ molecules are arrayed in an alternate fashion on a plane perpendicular to the molecular C_3 axis in an up-and-down arrangement to form an extended 2D puckered sheet structure with a hexanuclear unit (Fig. 4a). The two species are linked by imidazole–imidazolate hydrogen bonds. The intermolecular N···N hydrogen bond distances are in the range of 2.752(7) – 2.784(8) Å. The Fe–N distances of **3** reveal that all the iron ions of the $[Fe^{II}(H_3L)]^{2+}$ species (Fe1, Fe4, and Fe6) are HS Fe^{II}, and those of the $[Fe^{III}(L)]$ species (Fe2, Fe3, and Fe5) indicate that the iron ions at the Fe2 and Fe5 sites are LS Fe^{III}, while the iron ion at the Fe3 site is HS Fe^{III}. A side view of crystal structure of **3**

(Fig. 4b) reveals that there are three types of layers: the first layer consists of HS $Fe^{II}1$ and the HS $Fe^{II}4$ complexes, the second layer consists of LS $Fe^{III}2$ and LS $Fe^{III}5$ complexes, and the third layer consists of HS $Fe^{III}3$ and HS $Fe^{II}6$ complexes. Intermolecular hydrogen bonding connects the HS $Fe^{II}1$ and LS $Fe^{III}5$, HS $Fe^{II}6$ and LS $Fe^{III}2$, and HS $Fe^{II}4$ and HS $Fe^{III}3$ complexes. Each complex becomes chiral with either a Δ (clockwise) or Λ (anticlockwise) configuration due to the screw coordination arrangement of the achiral tripodal ligand around the Fe^{II} or Fe^{III} ion. The absolute configurations around the six iron atoms, Fe1–Fe6, are the same and **3** crystallizes in the acentric space group, *P*3. These facts indicate that spontaneous resolution takes place during the course of crystallization.

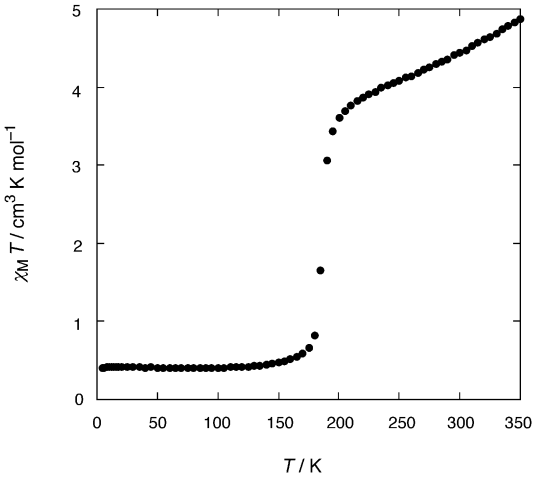

Fig. 5. A plot of $\chi_M T$ versus T for $[Fe^{II}(H_3L)][Fe^{III}(L)](BF_4)_2 \cdot 1.5H_2O$ (**3**)

The magnetic properties of **3** are represented in Fig. 5 in the form of a $\chi_M T$ versus T curve. In the temperature region of 2–150 K, $\chi_M T$ = 0.4 cm^3·K·mol^{-1}, and thus, in the range expected for LS states at both the Fe^{II} (S = 0) and Fe^{III} (S = 1/2) sites. The $\chi_M T$ value changes rather abruptly in the region of 170–200 K, indicating a spin transition at the Fe^{II} site. The value of $\chi_M T$ = 3.6 cm^3·K·mol^{-1} at 200 K, and is close to the calculated value for HS Fe^{II} (S = 2) and LS Fe^{III} states ($\chi_M T$ = 3.38 cm^3·K·mol^{-1}). Above 200 K, the value of $\chi_M T$ increases gradually due to the spin transition from LS to HS Fe^{III}. The value of $\chi_M T$ = 4.46 cm^3·K·mol^{-1} at 293 K is close to the calculated value ($\chi_M T$ = 4.71 cm^3·K·mol^{-1}) for HS Fe^{II} and a 2:1 mixture of LS and HS Fe^{III}, as determined by X-ray crystallography.

Mössbauer spectra were measured in the temperature range of 78–309 K. At 78 K, the Mössbauer spectrum consisted of two quadrupole-split doublets (LS Fe^{III}: δ = 0.19, ΔE_Q = 1.84, and LS Fe^{II}: δ = 0.42, ΔE_Q = 0.32 (mm·s^{-1})), demonstrating that both the Fe^{II} and the Fe^{III} sites were in the LS state. In the temperature range of 140–170 K, three doublets coexisted, because of the existence of LS and HS Fe^{II} sites

and LS Fe^{III} sites. The doublet arising from the LS Fe^{II} disappeared over 200 K. At 298 K, the absorption due to HS Fe^{III} was observed in addition to the absorptions of the HS Fe^{II} and LS Fe^{III}. Thus, the Mössbauer spectral results agree with the magnetic susceptibility results.

4. Conclusions

We have prepared $[Fe^{II}(H_3L)][Fe^{III}(L)](BF_4)_2 \cdot 1.5H_2O$ (**3**) with a supramolecular structure by a controlled deprotonation of $[Fe^{II}(H_3L)](BF_4)_2 \cdot 1.5H_2O$ (**2**) under aerobic conditions. In the supramolecular assembly of **3**, three independent properties are united: mixed-valence iron species, spin-crossover at the Fe^{II} and Fe^{III} sites, and the homochirality of the Fe^{II} and Fe^{III} building components. The magnetic properties of $[Fe^{II}(H_3L)](ClO_4)_2 \cdot 3H_2O$ (**1**) are quite different from those of the Fe^{II} species in **3**, demonstrating that the supramolecular association of the components into a mixed-valence material modifies their magnetic properties due to their co-operativity.

Acknowledgements

This work was supported by a Grant-in-Aid for Science Research (No. 14340209) from the Japanese Ministry of Education, Science, Sports, and Culture, from the Fund for Project Research from the Venture Business Laboratory of the Graduate School of Okayama University, and a JSPS Research Fellowship for Young Scientists (Y. S.).

References

[1] KAHN O., MARTINEZ C. J., Science, 279 (1998), 44.
[2] GÜTLICH P., HAUSER A., SPIERING H., Angew. Chem. Int. Ed. Engl., 33 (1994), 2024.
[3] HAYAMI S., GU Z.-Z., SHIRO M., EINAGA Y., SATO, O., J. Am. Chem. Soc., 122 (2000), 7126.
[4] VAN KONNINGSBRUGGEN P. J., GARCIA Y., KAHN O., FOURNES L., KOOIJMAN H., SPEK A. L., HAASNOOT J. G., MOSCOVICI J., PROVOST K., MICHALOWICZ A., RENZ F., GÜTLICH P., Inorg. Chem., 39 (2000), 1891.
[5] SORAI M., ENSLING J., HASSELBACH K. M., GÜTLICH, P., Chem. Phys., 20 (1977), 197.
[6] SUGIYARTO K. H., WEITZNER K., CRAIG D. C., GOODWIN H., Aust. J. Chem., 50 (1997), 869.
[7] ZHONG Z. J., TAO J.-Q., YU Z., DUN C.-Y., LIU Y.-J., YOU X.-Z., J. Chem. Soc., Dalton Trans, (1998), 327.
[8] LÉTARD J.-F. GUIONNEAU P., RABARDEL L., HOWARD J. A. K., GOETA A. E., CHASSEAU D., KAHN O., Inorg. Chem., 37 (1998), 4432.
[9] KATSUKI I., MOTODA Y., SUNATSUKI Y., MATSUMOTO N., NAKASHIMA T., KOJIMA M., J. Am. Chem. Soc., 124 (2002), 629.
[10] *Crystal Structure Analysis Package*, Rigaku and MSC (2001).
[11] BEATTIE, J. K., Adv. Inorg. Chem., 32 (1988), 1.
[12] BREUNING E., RUBEN M., LEHN J.-M., RENZ F., GARCIA Y., KSENOFONTOV V., GÜTLICH P., WEGELIUS E., RISSANEN K., Angew. Chem. Int. Ed. Engl., 39 (2000), 2504.
[13] SLATTERY S. J., BLAHO J. K., LEHNES J., GOLDSBY K. A., Coord. Chem. Rev., 174 (1998), 391.

Received 11 March 2003
Revised 26 March 2003